



**HAL**  
open science

## A new Aerodynamic traction principle for handling products on an Air Cushion.

Guillaume J. Laurent, Anne Delettre, Nadine Le Fort-Piat

► **To cite this version:**

Guillaume J. Laurent, Anne Delettre, Nadine Le Fort-Piat. A new Aerodynamic traction principle for handling products on an Air Cushion.. IEEE Transactions on Robotics, 2011, 27 (2), pp.379-384. 10.1109/TRO.2011.21092011 . hal-00601935

**HAL Id: hal-00601935**

**<https://hal.science/hal-00601935v1>**

Submitted on 21 Jun 2011

**HAL** is a multi-disciplinary open access archive for the deposit and dissemination of scientific research documents, whether they are published or not. The documents may come from teaching and research institutions in France or abroad, or from public or private research centers.

L'archive ouverte pluridisciplinaire **HAL**, est destinée au dépôt et à la diffusion de documents scientifiques de niveau recherche, publiés ou non, émanant des établissements d'enseignement et de recherche français ou étrangers, des laboratoires publics ou privés.

# A New Aerodynamic Traction Principle for Handling Products on an Air Cushion

Guillaume J. Laurent, Anne Delettre and Nadine Le Fort-Piat

**Abstract**—This paper introduces a new aerodynamic traction principle for handling delicate and clean products, such as silicon wafers, glass sheets or flat foodstuff. The product is carried on a thin air cushion and transported along the system by induced air flows. This induced air flow is the indirect effect of strong vertical air-jets that pull the surrounding fluid. The paper provides a qualitative explanation of the operating principles and a description of the experimental device. Very first experimental results with active control are presented. The maximum velocity and acceleration that can be obtained for the considered device geometry meet the requirements for industrial applications.

**Index Terms**—Contactless manipulation, Distributed manipulation.

## I. INTRODUCTION

Many industries require contactless transport and positioning of delicate or clean objects such as silicon wafers, glass sheets, solar cell or flat foodstuffs. The handling of delicate, freshly painted, hot, sensitive or micron-sized structured components is feasible because mechanical contact is avoided. Contamination from and of the end-effector can be totally avoided. This can be important in food handling or in semiconductor production processes. Furthermore, dry friction forces are canceled, which enables accurate positioning or high velocity motions.

In order to avoid contact between feeding devices and work pieces, many handling approaches have been proposed. These methods typically employ magnetic, electrostatic, near-field and aerodynamic levitation [14]. Both magnetic and electric levitation are restricted to conductive materials and the lifting force depends on material properties. Pneumatic levitation approaches use air flow to apply a force to a work piece. Because air flow is magnetic free and generates little heat, pneumatic approaches can be applied to any material: insulator or conductor, magnetic or non-magnetic, rigid or non-rigid.

Researchers have experimented with a variety of air-jet techniques to design contactless manipulators. Aerodynamic levitation uses a flow of gas to apply a lift force. Two different approaches can be considered: air cushion or Bernoulli levitation. In Bernoulli levitation, the sample is held below the end-effector of the manipulator which consists in a cup-shaped air nozzle [17]. Bernoulli levitation has been used in practical applications to “pick-and-place” wafers [8] and flat soft foodstuffs [4].

In air cushion levitation, the sample is held on a plate which is drilled by many small holes. Pressurized air flows upwards through these holes and creates an air cushion that counterbalances the weight of the component. This is the principle of popular air-hockey tables. Two additional means have been proposed to move the object: suction and tilted air jets.

Luntz and Moon [9], [11], [15], [16] use an air-hockey table in addition to a few flow sinks (suction points) above the table. The sinks create a stable flow pattern towards them. This device is a sensorless positioning surface able to move any rectangular object to a predictable orientation and position. Ku *et al.* [7] developed the same idea but they used closed-loop control to move the object from

Manuscript received March 26, 2010. This work was supported in part by the Smart Surface NRA (French National Research Agency) project (ANR\_06\_ROBO\_0009).

G. J. Laurent, A. Delettre and N. Le Fort-Piat are with the Automatic Control and Micro-Mechatronic Systems Department, FEMTO-ST Institute, UFC-ENSMM-UTBM-CNRS, Université de Franche-Comté, Besançon, France, corresponding author: guillaume.laurent@ens2m.fr

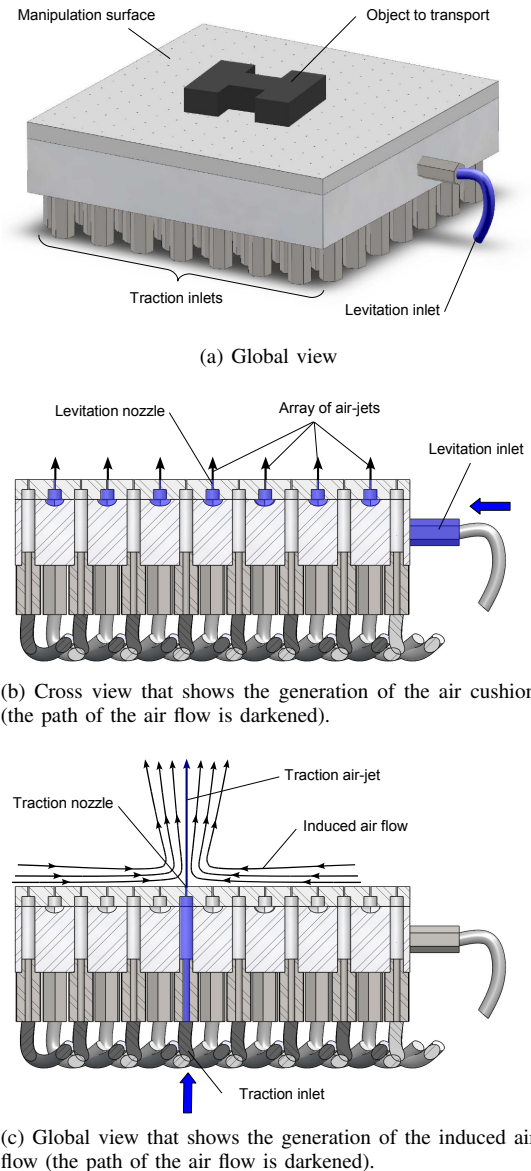


Figure 1. The induced air flow surface.

one sink to another. The device is a  $4 \text{ mm} \times 4 \text{ mm}$  array of 100 capillary glass tubes. Each tube is equipped with a pressure sensor and a two-position valve which provides positive or negative pressures. The typical velocity of the object is  $8 \text{ mm}\cdot\text{s}^{-1}$ .

Many devices use arrays of tilted air-jets to produce a traction force in addition to the air cushion. The geometry of the device is designed to get stable transport system without closed-loop control, for example we can mention wafer and glass transportation systems [1], [6], [12]. In contrast, the Xerox PARK paper handling system [2], [3] uses 1,152 directed air-jets in a 12 in.  $\times$  12 in. array to levitate paper sheets. Each jet is separately controlled by an independent MEMS-like valve. 32,000 optical sensors (photodiodes) are integrated between actuators to sense and control the paper position. The levitation-transport system uses two arrays of 578 valves arranged in opposition to one another across a small gap in which the paper is located. The system has demonstrated closed-loop positioning accuracies in the order of 0.05 mm and trajectory tracking with typical velocity about  $30 \text{ mm}\cdot\text{s}^{-1}$ . Rij *et al.* [13] proposed a wafer transport system based on viscous traction

principle. The device is designed to produce horizontal air flow under the wafer. The principle is then similar to the paper handling system. On a near microscopic scale, some active surfaces have been developed using MEMS actuator arrays. The surface of Fukuta et al. [5] is able to produce tilted air-jets thanks to integrated electrostatic valves. In their experiments a flat plastic piece was successfully moved with velocity about  $4.5 \text{ mm}\cdot\text{s}^{-1}$ .

This paper introduces a new principle to move an object on an air-hockey table. This system use neither tilted air jet nor suction nozzle. The object is moved indirectly by an air flow which is induced by some strong vertical air jets. These strong jets are coming from some specific orifices of the air-hockey table.

This paper is organized as follow. The first part presents a qualitative explanation of the operating principles and a description of the experimental device called induced air flow surface. The second part describes the active control of the device. The last parts present first experimental results, their analysis and future works.

## II. INDUCED AIR FLOW SURFACE

The induced air flow surface is a  $120 \text{ mm}\times 120 \text{ mm}$  square surface upon which an object is moving in aerodynamic levitation.

The device consists of two parts detailed in the exploded view of the Figure 1:

- the upper-block is drilled of  $15 \times 15$  holes (nozzles); each one is  $0.4 \text{ mm}$  in diameter;
- the lower-block is drilled of 112 holes in staggered rows; these holes connect one nozzle out of two to independent air inlets; these nozzles are useful to create induced air flow; between the holes of the lower-block a network of diagonal channels connects the other nozzles to a common air inlet located on the side; the airflow spreads over this network and creates the air cushion under the object.

The object is maintained in constant levitation thanks to the air cushion created by the airflow that comes through the common air inlet (cf. Figure 1b). *The novelty is that the object can be moved on the table by generating strong vertical air-jets through the specific nozzles of the surface.* Each nozzle is driven by an independent solenoid valve (3/2 normally closed valve). When a valve is open, air-flow comes through both blocks and generates a vertical air-jet on the front side of the upper-block. The air-jet creates an induced air flow in the surrounding fluid that pulls the object towards the nozzle (cf. Figure 1c). This traction phenomena is a counter-intuitive physics demonstration of fluid mechanics such as the popular Bernoulli levitation [17]. It would be very interesting in future works to describe it in a more formal and quantitative way.

The experimental setup for the distributed-air-jet manipulator is composed of pressurized air supply, two pressure regulators, the set of solenoid valves and its control system, and a computer for vision processing. Figures 2 and 3 describe the complete hardware configuration.

The induced air flow surface is put on a mechanical platform to adjust its equilibrium position. The air-flow source is provided by compressed air *via* two pressure control systems. One regulator controls the levitation and the other one supplies air pressure for the valves. Default settings for operating pressures are  $10 \text{ kPa}$  for levitation and  $500 \text{ kPa}$  for traction.

Each valve is independently actuated by an electric signal. The electrical voltage applied to the valves is  $24 \text{ V DC}$ . Control signals are sent by computer *via* a multi-channel digital output board (NI USB-6509) and a  $5\text{V}/24\text{V}$  amplifier circuit.

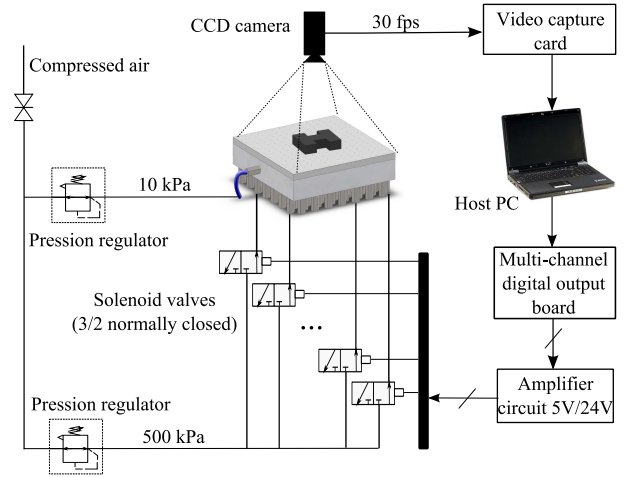


Figure 2. Complete hardware configuration.

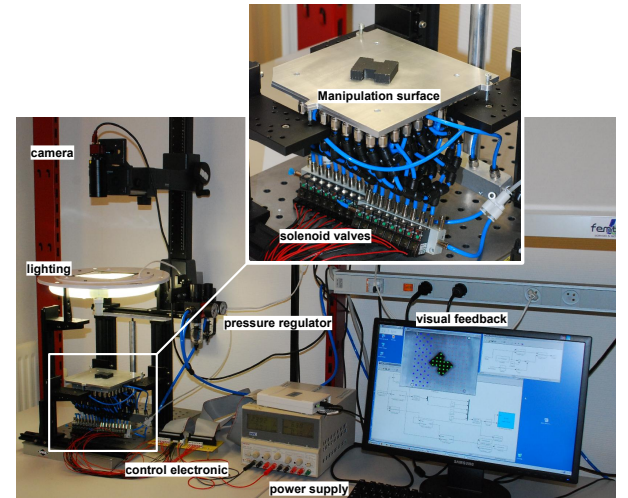


Figure 3. Overview of the experimental setup.

A camera is used to grab video frames of the surface of the manipulator. The image processing is done by a computer at the rate of 30 frames per second (the software is cvLink).

## III. ACTIVE CONTROL

Contrary to the device of Luntz and Moon, the induced air flow principle does not create stable equilibrium positions and then can not operate without active control. Actually the induced air flow pulls the object towards the nozzle and when the object masks the orifice, the air jet is over. In this case the air radially flows outwards. While the nozzle is under the object, this one is free to move in any direction.

So to control the induced air flow surface, we need sensors. With the aim to conduct the proof-of-concept of a future surface integrating sensors under each nozzle, we emulate local sensors thanks to the image of the camera. The image processing calculates the state  $b_i(k)$  of every emulated sensor  $i$  for each frame  $k$ .  $b_i(k)$  is 1 if the object is above the nozzle  $i$  and 0 else. Figure 4 shows the working of the sensor emulation.

The state  $b_i(k)$  of the sensors is sent to the valve controllers. Then, the controllers independently allocate a state  $u_i(k)$  to each valve  $i$  so as to generate a specific motion of the object.  $u_i(k) = 1$  means that the valve  $i$  is open at time  $k$ ,  $u_i(k) = 0$  means that the valve is closed.

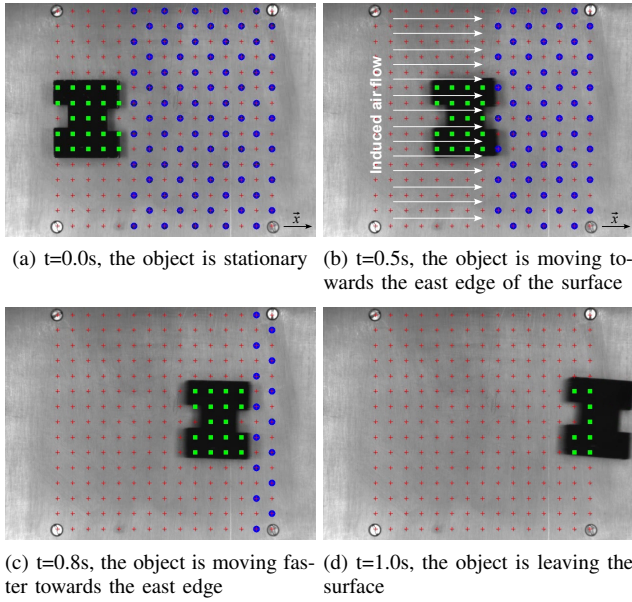


Figure 4. Image sequence of an experiment with a H-shaped object (dark crosses represent inactive sensors, light squares represent active sensors and dark circles represent active traction nozzles).

The long term objective with this system is to control three degrees of freedom of an object (two directions and one angle). In this paper, we focus on 1D-control for doing first experiments and establishing a model of the system. The task is to send the object towards the east edge of the surface. For this task, the control laws are quite simple. To carry the object to the east, the valve located east of the object must be opened.

We note  $x_i$  the abscissa of the nozzle linked to the valve  $i$ . The control law  $u_i(k)$  of an air-jet is defined by:

$$u_i(k) = \begin{cases} 1 & \text{if } x_i > x_{max}(k) \\ 0 & \text{else} \end{cases} \quad (1)$$

where  $x_{max}(k)$  is abscissa of the eastern active sensor at time step  $k$ .

$$x_{max}(k) = \max_{i, b_i(k)=1} x_i \quad (2)$$

#### IV. EXPERIMENTS

##### A. Acceleration trial

In this section, we report very first experimental results obtained with the induced air flow surface. To begin with, we used a H-shaped object made of aluminum piece (mass: 32.38 g, dimension: 39 mm×33 mm×9 mm). A trial starts by placing the object against the west edge on the surface. Thanks to the virtual sensors, the controller opens the appropriate valves that induces an air flow towards the east and moves the object. Figure 4 shows an image sequence extracted from a video made during the experimental manipulation, which can be further appreciated in the video clip accompanying this paper<sup>1</sup>.

Figure 5 shows the trajectory of the H-shaped object for different values of traction pressure. The exit velocity increases with the pressure from 89 to 181 mm·s<sup>-1</sup> whereas the time response decreases.

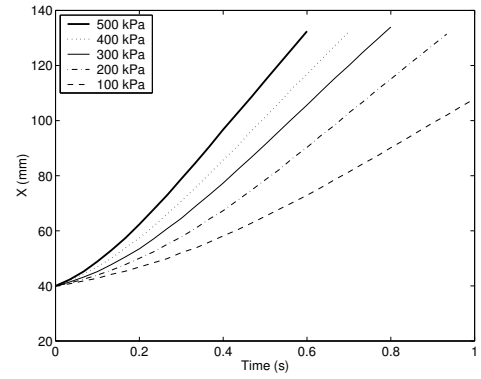


Figure 5. Abscissa of the center of the object according to time for different traction pressures. The valves are opened at time 0.

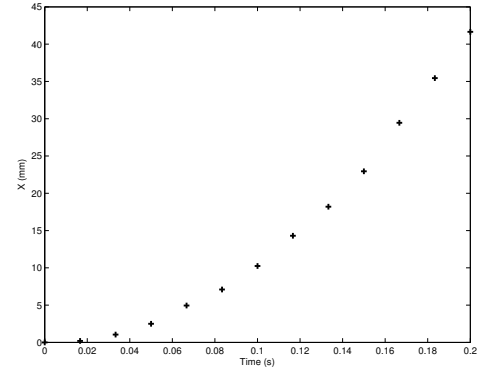


Figure 6. Position of a small polystyrene ball of negligible mass according to time. The valves are opened at time 0.

##### B. Dynamic model

To a first approximation, we can assume that the object receives two forces, a viscous traction due to the induced air flow and a viscous drag force due to friction of the air cushion on its backside:

$$m\ddot{x}(t) = k_t[v_{air}(t) - \dot{x}(t)] - k_d\dot{x}(t) \quad (3)$$

where  $m$  is the mass of the object,  $v_{air}$  is the velocity of the induced air flow,  $k_t$  is the viscous traction coefficient corresponding to the front and lateral sides of the object and  $k_d$  another viscous coefficient corresponding to the backside of the object.

In other words, the motion of the object is described by a first order model with integrator:

$$\frac{X(s)}{V_{air}(s)} = \frac{\frac{k_t}{k_t+k_d}}{s(1 + \frac{m}{k_t+k_d}s)} = \frac{K_o}{s(1 + \tau_o s)} \quad (4)$$

The velocity of the induced air flow depends on time. To measure it, we use small expanded polystyrene balls of negligible mass. By opening the valves, the ball moves with the air jet and its velocity is approximately the same as the air flow thanks to its negligible mass.

By observing the position of the balls for a step response (see Figure 6) and deducing the air velocity we can model the induced air flow dynamic by a first order:

$$\frac{V_{air}(s)}{P(s)} = \frac{K_a}{1 + \tau_a s} \quad (5)$$

where  $P(s)$  is the Laplace variable corresponding to the input pressure  $p$ ,  $K_a$  is the gain, and  $\tau_a$  the time constant corresponding

<sup>1</sup>Also available at <http://www.femto-st.fr/~guillaume.laurent/>

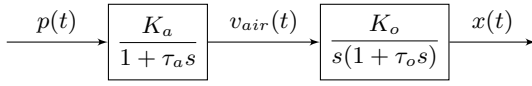


Figure 7. Dynamic model of the system.

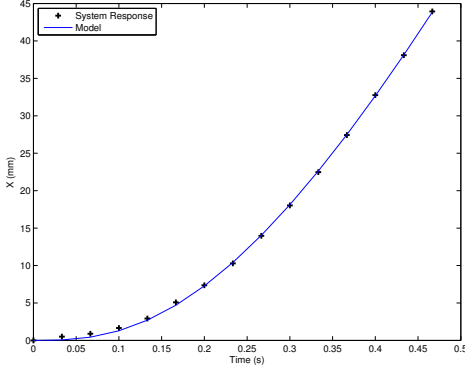


Figure 8. Comparison between the model and the experimental data. The reference signal is a step of amplitude 500 kPa.

to the establishment of the induced air flow, including the dynamic of the valves.

Figure 7 shows the proposed model of the global system.

### C. Parameters identification

The experimental identification of the gain  $K_a$  and the time constant  $\tau_a$  is done using a mean square error minimization in the time domain. The gain and the time constant depend on the pressure value. Actually the system is not linear according to the input pressure. For a traction pressure of 500 kPa we obtain  $K_a = 0.742 \text{ mm}\cdot\text{s}^{-1}\cdot\text{kPa}^{-1}$  and  $\tau_a = 0.085 \text{ s}$ . The maximum velocity of the air is  $371 \text{ mm}\cdot\text{s}^{-1}$ .

The characterization of the viscous friction coefficients can be established by the velocity measured during the acceleration phase for the conveyed object (cf. Figure 5). We obtain  $k_t = 83.04 \text{ mN}\cdot\text{m}^{-1}\cdot\text{s}$  and  $k_d = 56.53 \text{ mN}\cdot\text{m}^{-1}\cdot\text{s}$ . The comparison between the system response and the model output for a step reference signal of amplitude 500 kPa is shown on Figure 8.

### D. Estimated performances

The model of the device can be used to do simulations and estimate its expected performances. For instance, we can estimate the maximum velocity that the object could reach with a long enough active surface. The maximum velocity is  $K_a * K_o * p$ . For the H-shaped object the maximum velocity the object could reach is  $220 \text{ mm}\cdot\text{s}^{-1}$  with a traction pressure of 500 kPa.

The settling time of the steady state of the system is given by (for 5%):

$$T_s = \frac{3}{\omega_0(\xi - \sqrt{\xi^2 - 1})} \quad (6)$$

with  $\omega_0 = 1/\sqrt{\tau_a * \tau_o}$  and  $\xi = (\tau_a + \tau_o)/2\sqrt{\tau_a * \tau_o}$ .

The settling time for the H-shaped object is 0.70 s.

We can also estimate the maximum traction force that the induced air flow is able to produce. The traction force is given by:

$$F_t(t) = k_t(v_{air}(t) - \dot{x}(t)) \quad (7)$$

Figure 9 shows the estimated traction force according to time. The traction force starts from zero because of the settling time of

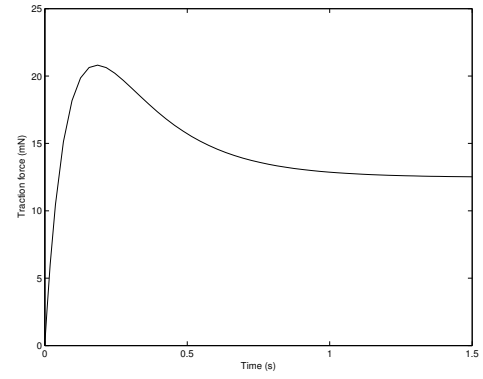


Figure 9. Estimated traction force of the H-shaped object according to time. The valves are opened at time 0.

the induced air flow. When the air flow is established and when the object still moves slowly, the traction force reaches a maximum value. Then, the traction force reduces after that time since its value depends on the difference of velocities between the air flow and the object. The peak is reached 0.185 s after the opening of the valves and is about 20.81 mN in value.

We carried out some experiments with different kinds of objects. The results are reported in Table I. The device works better with large and thick objects: the velocity of the object and the traction force are larger, and the settling time is smaller. It is obvious because large and thick objects have a higher drag coefficient that makes the traction more efficient. Furthermore the backside of object must be flat. Indeed, a rough face leads to use higher levitation pressure that is only possible with heavy objects.

## V. DISCUSSION

Compared to existing devices, the induced air flow surface produces traction forces in the range of other techniques using tilted air-jets. The tests show that this system is able to produce a force from 1 mN to 21 mN depending on the shape of the object. For instance, the Berlin's Xerox PARK paper handling system [2], [3] exerts a force about 10 mN on a  $15 \text{ cm} \times 13 \text{ cm}$  plastic sheet. The simulations of the viscous traction concept of Rij et al. [13] predict a force up to 18 mN on a 100 mm silicon wafer.

In terms of velocity, the induced air flow surface outperforms the existing devices even for thin products. But one negative point is the energetic efficiency. Since the actuation is indirect, only a small part of the mechanical potential energy of the pressured air is used to move the object. Nevertheless, this fact is balanced by the absence of dry friction.

Concerning the bandwidth, our device is in the middle range. It is faster than Luntz and Moon's system one but slower than the devices which use MEMS valves like Fukuta's [5] and Berlin's ones. Contrary to these last systems, the induced air flow surface requires only conventional technologies and conventional machining that are cheaper and more robust. In addition, both Luntz's and Berlin's devices are limited to flat product since the object is moved between two opposite plates. In our case, the upper space is free. The induced air flow surface can manipulate thick objects and enables the access for a robot to pick or place objects on the surface.

About the controllability of the object motion, this paper presents experiments in a single direction. But, this traction principle is able to control the three degrees of freedom of the object on the plan (two translations and one rotation). Actually, the traction air jets acts like suction points in the surrounding air. By selecting the right air-jets,

Object description	Size L×W×H (mm)	Mass (g)	Levitation pressure (kPa)	Traction pressure (kPa)	Exit velocity (mm·s <sup>-1</sup> )	Estimated settling time (s)	Estimated maximum velocity (mm·s <sup>-1</sup> )	Estimated maximum traction force (mN)
H-shaped object	39 × 33 × 9	32.38	10	500	181	0.69	220	20.81
A chocolate	28 × 26 × 11	9.08	35	500	339	0.25	355	17.73
After Eight chocolate	40 × 40 × 4	8.61	5	500	183	0.79	215	4.94
2.5" Hard disk	∅64 × 0.675	4.79	5	500	104	1.46	124	1.04
Metal plate	45 × 30 × 0.4	3.56	15	500	118	1.46	184	0.99
Fragment of silicon wafer	25 × 20 × 0.29	0.28	5	100	120	-	-	-
Business card	87 × 50 × 0.39	1.51	5	200	113	-	-	-

Table I  
EXPERIMENTS WITH DIFFERENT OBJECTS.

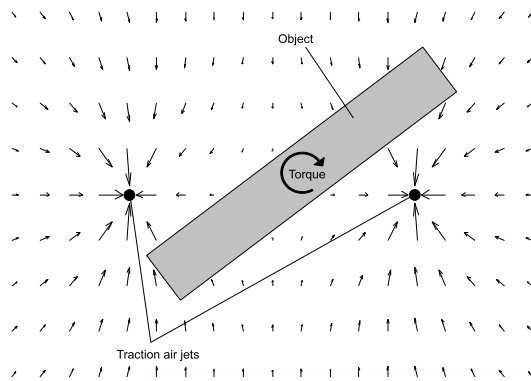


Figure 10. Two traction air jets form a useful induced air flow (top view).

we can induce an air flow that exerts a force and also a torque on an elongated object. Figure 10 illustrates the rotation capability by opening two traction nozzles.

## VI. CONCLUSION AND FUTURE WORK

The described new contactless transport system for delicate and clean products may be implemented in several industrial production processes, such as semiconductor manufacturing, flat panel display production equipment, solar cell production or food industry, etc. The results indicate that the traction force and the bandwidth of the considered device are sufficient when compared with requirements for possible industrial applications.

These experiments are a proof-of-concept that demonstrates the potentiality of the principle. In the future, more complex tasks could be achieved such as 3-dof positioning, trajectory following, part sorting, etc. These tasks require independent control of each traction nozzle. Finding coherent control laws for hundreds of independent air jets is a challenging problem [10]. With this aim in view, a distributed model of the device behavior would be very useful to predict the motion in presence of multiple air jets.

Another great challenge is to integrate the sensors, the valves and the control circuits inside the surface. In this paper, we used a video camera to emulate local sensors and a PC to calculate the control laws. The long term objective is to integrate distributed control units to get a flexible, scalable and robust contactless transport device.

## ACKNOWLEDGMENTS

The authors gratefully acknowledge Joël Agnus and David Guibert from the FEMTO-ST Institute for their technical assistance.

## REFERENCES

- [1] J. P. Babinski, B. I. Bertelsen, K. H. Raacke, V. H. Sirgo, and C. J. Townsend. Transport system for semiconductor wafer multiprocessing station system. U. S. Patent 3,976,330, 1976.
- [2] A. Berlin, D. Biegelsen, P. Cheung, M. Fromherz, D. Goldberg, W. Jackson, B. Preas, J. Reich, and L.-E. Swartz. Motion control of planar objects using large-area arrays of mems-like distributed manipulators. *Micromechatronics*, 2000.
- [3] D. K. Biegelsen, A. Berlin, P. Cheung, M. P.J. Fromherz, D. Goldberg, W. B. Jackson, B. Preas, J. Reich, and L.-E. Swartz. Air-jet paper mover: An example of meso-scale mems. In *SPIE Int. Symposium on Micromachining and Microfabrication*, 2000.
- [4] S. Davis, J.O. Gray, and Darwin G. Caldwell. An end effector based on the bernoulli principle for handling sliced fruit and vegetables. *Robotics and Computer-Integrated Manufacturing*, 24:249–257, 2008.
- [5] Y. Fukuta, Y.-A. Chapuis, Y. Mita, and H. Fujita. Design, fabrication and control of mems-based actuator arrays for air-flow distributed micromanipulation. *IEEE/ASME Journal of Microelectromechanical Systems*, 15(4):912–926, 2006.
- [6] M. Hoetzle, T. Dunifon, and L. Rozevink. Glass transportation system. U.S. Patent 6,505,483, 2003.
- [7] P.-J. Ku, K. Tobias Winther, and H. E. Stephanou. Distributed control system for an active surface device. In *Proc. of the IEEE Int. Conf. on Intelligent Robots and Systems*, pages 3417–3422, 2001.
- [8] X. Li, K. Kawashima, and T. Kagawa. Analysis of vortex levitation. *Experimental Thermal and Fluid Science*, 32:1448–1454, 2008.
- [9] J. Luntz and H. Moon. Distributed manipulation with passive air flow. In *Proc. of the IEEE Int. Conf. on Intelligent Robots and Systems*, pages 195–201, 2001.
- [10] L. Matignon, G. J. Laurent, N. Le Fort-Piat, and Y.-A. Chapuis. Designing decentralized controllers for distributed-air-jet mems-based micromanipulators by reinforcement learning. *Journal of Intelligent and Robotic Systems*, 59(2):145–166, 2010.
- [11] H. Moon and J. Luntz. Distributed manipulation of flat objects with two airflow sinks. *IEEE Transactions on robotics*, 22(6):1189–1201, 2006.
- [12] J. A. Paivanas and J. K. Hanssan. Wafer air film transportation system. U.S. Patent 4,081,201, 1978.
- [13] J. van Rij, J. Wesselingh, R. A. J. van Ostayen, J.W. Spronck, R.H. Munnig Schmidt, and J. van Eijk. Planar wafer transport and positioning on an air film using a viscous traction principle. *Tribology International*, 42:1542–1549, 2009.
- [14] V. Vandaele, P. Lambert, and A. Delchambre. Non-contact handling in microassembly: Acoustical levitation. *Precision Engineering*, 29:491–505, 2005.
- [15] K. Varsos and J. Luntz. Superposition methods for distributed manipulation using quadratic potential force fields. *IEEE Transactions on robotics*, 22(6):1202–1215, 2006.
- [16] K. Varsos, H. Moon, and J. Luntz. Generation of quadratic potential force fields from flow fields for distributed manipulation. *IEEE Transactions on robotics*, 22(1):108–118, 2006.
- [17] C. Waltham, S. Bendall, and A. Kotlicki. Bernoulli levitation. *American Journal of Physics*, 71(2):176–179, 2003.